Studies on the field-induced martensite to austenite phase transition in $Ni_{50}Mn_{34}In_{16}$ alloy

2008 J. Phys.: Condens. Matter 20 425210

(http://iopscience.iop.org/0953-8984/20/42/425210)

J. Phys.: Condens. Matter **20** (2008) 425210 (7pp) doi:10.1088/0953-8984/20/42/425210

Studies on the field-induced martensite to austenite phase transition in $Ni_{50}Mn_{34}In_{16}$ alloy

V K Sharma, M K Chattopadhyay and S B Roy

Magnetic and Superconducting Materials Section, Raja Ramanna Centre for Advanced Technology, Indore 452013, India

Received 25 June 2008, in final form 6 August 2008
Published 25 September 2008
Online at stacks.iop.org/JPhysCM/20/425210

Abstract

The magnetic transition coupled with the martensitic transition in $Ni_{50}Mn_{34}In_{16}$ alloy is studied through magnetization measurements. The field-induced martensite to austenite transition has been studied in detail, and the method of using inverted Arrott's plots (H/M versus M^2 plots) to distinguish between the first- and second-order magnetic phase transitions is found to be inadequate in the present case. The temperature dependence of the characteristic magnetic fields for the field-induced first-order martensite to austenite phase transition in $Ni_{50}Mn_{34}In_{16}$ is also found to be different from the field-induced first-order paramagnetic to ferromagnetic phase transition observed in other systems. These observations are explained in the framework of disorder-broadened first-order phase transition.

(Some figures in this article are in colour only in the electronic version)

1. Introduction

Traditionally, Arrott's plots (M^2 versus H/M plots, where H is the applied magnetic field and M is the measured magnetization of a sample) are used to analyse the ferromagnetic character of a material [1]. It has also been shown theoretically [2] that the sign of the slope of the H/M versus M^2 isotherms may be employed to distinguish between the first- and second-order magnetic phase transitions. It was found that a positive slope of the H/M versus M^2 isotherm is related to the second-order magnetic transition, while a negative slope corresponds to the first-order magnetic transition. This criterion [2] has been employed for the identification of the order of the magnetic transitions in MnAs [2], various manganite systems [3–7] and Ru-doped $CeFe_2$ [8]. The same criterion has also been used to investigate the magnetic transitions in the ferromagnetic shape memory alloy system NiMnGa [9].

The off-stoichiometric $Ni_{50}Mn_{50-x}In_x$ alloys are currently attracting considerable attention because of their potential as ferromagnetic shape memory alloys [10–12, 14]. The phase diagram of this alloy system depicts that these alloys undergo a first-order transition from the austenite phase to the martensite phase with the lowering of temperature [10]. Further, the reverse transition, i.e. the martensite to austenite transition in this alloy system, can be induced both by temperature and magnetic field [10–19]. The alloy $Ni_{50}Mn_{34}In_{16}$ exhibits a paramagnetic to ferromagnetic transition around 305 K, followed by an austenite to martensite transition around 220 K [10, 12–19]. In the temperature regime of the field-induced first-order martensite to austenite phase transition [13–18], the alloy shows large magnetoresistance [13, 14], large magnetocaloric effect [15–17] and magnetic superelasticity [16]. In the present work, we perform a detailed investigation of this field-induced martensite to austenite phase transition by studying H/M versus M^2 isotherms. We show that, though the martensitic transition in this alloy is first order in nature, the criterion of negative slope of the H/M versus M^2 isotherms is not strictly applicable here. It is found that, instead of a negative slope, a decrease of slope is observed in some of the isothermal H/M versus M^2 curves in the temperature regime of the field-induced martensite to austenite phase transition. The temperature dependence of the characteristic fields associated with this phase transition is also analysed in detail.

2. Experimental details

The polycrystalline sample with the nominal composition $Ni_{50}Mn_{34}In_{16}$ was prepared by arc melting of pure elements

in an argon gas atmosphere. The sample was flipped and re-melted several times to ensure homogeneity. The sample was characterized in an x-ray diffraction (XRD) study. At room temperature, the sample was found to have an $L2_1$ structure. The actual composition of the sample was determined to be $Ni_{49.2}Mn_{34.7}In_{16.1}$ by energy-dispersive x-ray analysis (EDX). Portions of this sample were used for other works reported recently [14, 15, 18, 19]. The magnetization (M) measurements as a function of temperature (T) and magnetic field (H) were performed using a commercial superconducting quantum interface device (SQUID) magnetometer (MPMS-5; Quantum Design) and a vibrating sample magnetometer (VSM, Quantum Design).

3. Results and discussion

3.1. Temperature dependence of magnetization

Figure 1 presents the $M(T)$ curves of $Ni_{50}Mn_{34}In_{16}$ alloy measured in a field of 10 kOe in the field-cooled cooling (FCC) and field-cooled warming (FCW) protocols. These results have been reported earlier [15] but are included here for completeness. The paramagnetic to ferromagnetic transition around 305 K and the hysteretic martensitic transition below 250 K are clearly observed in figure 1. The nature of variation of $M(T)$ in the temperature regime away from the austenite–martensite phase transition indicates that both austenite and martensite phases are ferromagnetic in nature. The insets to figure 1 show the variation of the saturation magnetization (in 50 kOe magnetic field) as a function of T in the martensite (inset (a)) and austenite (inset (b)) phases. The fitted lines in insets (a) and (b) represent equation (1) which is the characteristic function of a ferromagnet as proposed by Kuz'min *et al* [20, 21]

$$M(T) = M(0)\left[1 - s\left(\frac{T}{T_C}\right)^{3/2} - (1-s)\left(\frac{T}{T_C}\right)^{5/2}\right]^{1/3}. \quad (1)$$

In equation (1) $M(T)$ is the spontaneous magnetization at temperature T, $M(0)$ is the spontaneous magnetization at $T = 0$ K and T_C is the Curie temperature. Also, s is the shape parameter that depends on the shape of the $M(T)$ curve and is related to the spin wave stiffness coefficient [20]. Equation (1) reduces to Bloch's law in the limit $T/T_C \to 0$ and gives the critical behaviour of the Heisenberg model in the limit $T/T_C \to 1$ [20]. However, in figure 1, we have fitted the experimentally measured saturation magnetization with equation (1). This does not lead to any qualitative error in understanding, as the fitted temperature regimes (insets (a) and (b) of figure 1) are well below the T_Cs of the respective phases (the T_Cs determined from the curve fitting is 237.36 K in the martensite phase and 311.06 K in the austenite phase).

The sharp change in M across the martensitic transition and the associated thermal hysteresis indicate that the transition is of first order in nature [22, 23]. Figure 1, along with the insets, also indicate that the saturation magnetization in the high T austenite phase is much higher than that in the low T martensite phase. The probable reason for the

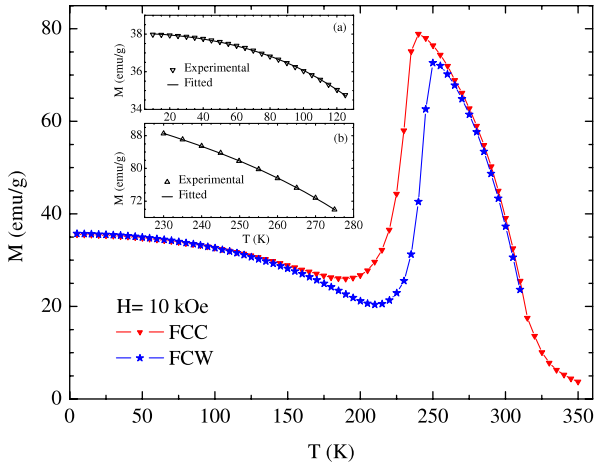

Figure 1. Temperature (T) dependence of magnetization (M) for $Ni_{50}Mn_{34}In_{16}$ alloy in 10 kOe magnetic field. The inset shows the fitting of the temperature dependence of saturation magnetization, in 50 kOe magnetic field, in the martensite (a) and austenite (b) phases with the characteristic function of a ferromagnet [20, 21].

sharp change in M across this transition is the change in exchange interaction because of the lattice change involved in the martensitic transition [24]. It is worth noting here that there is an excess of Mn in the off-stoichiometric composition $Ni_{50}Mn_{34}In_{16}$ as compared to the stoichiometric Ni_2MnIn. This leads to the occupation of a number of 4(b) sites in the $L2_1$ structure by Mn atoms [16, 25]. An incipient antiferromagnetic coupling exists between the magnetic moments of these extra Mn atoms [16, 25]. This antiferromagnetic coupling probably becomes stronger in the martensite phase [16, 25], though both the martensite and austenite phases retain their overall ferromagnetic character. This provides a probable explanation for the lower magnetization in the martensite phase. We shall now concentrate only on the field-induced first-order martensite to austenite phase transition.

3.2. Field dependence of magnetization

Figure 2 presents selected isothermal M versus H curves for the present $Ni_{50}Mn_{34}In_{16}$ alloy. For each isothermal $M(H)$ measurement, the sample was first warmed up to 300 K and then cooled down to the temperature of interest in zero applied magnetic field. This was followed by the measurement of magnetization with field increasing up to 80 kOe and then decreasing down to zero. Away from the temperature regime of the martensitic transition, the isothermal $M(H)$ curves are that of a soft ferromagnet (see the M–H curves at 5 and 260 K in figure 2) and show no hysteresis. But the isothermal $M(H)$ curves in the temperature regime of the martensitic transition show an additional rise in M above a critical H. This second rise in M is also associated with a field hysteresis. This hysteresis is quite different from that observed in a hard ferromagnet. In a ferromagnetic material the hysteresis arises due to domain wall pinning and/or anisotropy and has maximum width at $H = 0$. In such a case the width of the hysteretic region increases with the lowering of temperature. But in the present case the hysteresis is almost

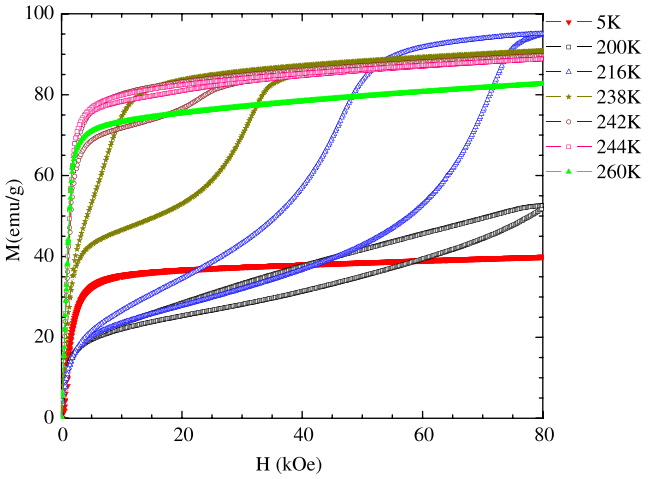

Figure 2. Isothermal magnetization (M) versus field (H) curves of $Ni_{50}Mn_{34}In_{16}$ alloy at representative temperatures.

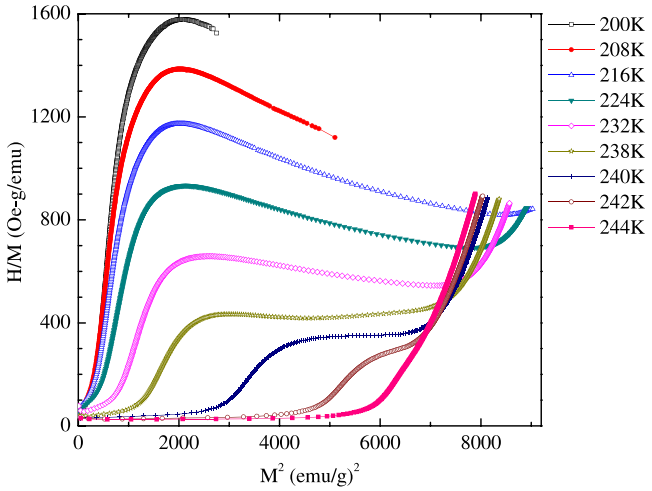

Figure 3. Isothermal H/M versus M^2 plots at representative temperatures across the martensitic transition in $Ni_{50}Mn_{34}In_{16}$ alloy.

zero at $H = 0$. Further the hysteresis vanishes both on the lower and higher temperature sides of the martensitic transition regime. The distinct rise in M with increasing H and the associated hysteresis mentioned above are typical signatures of a field-induced first-order magnetic transition and have been observed in various magnetic systems including MnAs [26], $HoNi_2B_2C$ [27], Gd_5Ge_4 [28], doped Mn_2Sb [29] and doped $CeFe_2$ alloys [30–32]. In the present $Ni_{50}Mn_{34}In_{16}$ alloy these features signify a field-induced first-order transition from the martensite to the austenite phase. Figure 2 shows that at 200 K the field-induced transition is not complete up to 80 kOe magnetic field. In the same field value the field-induced transition is near to completion at 216 K. At 244 K the change in M across the field-induced martensite to austenite transition is very small, and so is the associated field hysteresis. The typical signatures of the field-induced martensite to austenite phase transition mentioned above are observed more clearly in the $M(H)$ curves in the T regime 200–242 K (see figure 2).

3.3. H/M versus M^2 plots

Figure 3 shows representative H/M versus M^2 curves of the $Ni_{50}Mn_{34}In_{16}$ alloy across the austenite to martensite transition (200–244 K). The H/M versus M^2 curves were drawn using the increasing field portions of the isothermal $M(H)$ curves. The negative slope region in the H/M versus M^2 curves in the temperature range 200–238 K corresponds to the portion of the $M(H)$ curves that represent a field-induced first-order martensite to austenite phase transition. But in the temperature range 240–244 K, though the isothermal $M(H)$ curves depict the signatures (explained in section 3.2) of a field-induced first-order martensite to austenite phase transition (figure 2), the H/M versus M^2 isotherms do not exhibit any negative slope. In this temperature regime, a decrease of slope of the H/M versus M^2 curves is found to correspond to the field-induced first-order martensite to austenite phase transition.

It has been shown theoretically that in systems undergoing a field-induced first-order paramagnetic to ferromagnetic transition, the slope of the H/M versus M^2 curves should be negative [2]. The negative slope of H/M versus M^2 isotherms in such systems is found to decrease gradually as T approaches the zero-field transition temperature [3–7]. Such a decrease in the magnitude of the negative slope of H/M versus M^2 isotherms is also observed across the field-induced first-order antiferromagnetic to ferromagnetic phase transition [8]. On the other hand, the absence of negative slope of H/M versus M^2 isotherms across a field-induced first-order magnetic transition, as observed here, is also visible in certain compositions of ferromagnetic shape memory alloy Ni–Mn–Ga [9], and in another member of the Ni–Mn–In alloy system, namely $Ni_{50}Mn_{35}In_{15}$ [33]. In Ni–Mn–Ga, as the temperature approaches a characteristic temperature, the negative slope of the H/M versus M^2 curves changes to a decrease of slope with an overall positive value across a paramagnetic to ferromagnetic phase transition (see [9] and figure 5(a) therein) as well as a ferromagnetic to ferromagnetic phase transition (see [9] and figure 3(a) therein).

3.4. Characteristic fields and temperatures of the field-induced martensite to austenite phase transition

Instead of using the H/M versus M^2 plots, the first-order austenite–martensite phase transition in the present $Ni_{50}Mn_{34}In_{16}$ alloy may be investigated in another way: we examine the temperature and field dependence of various characteristic parameters related to the first-order austenite–martensite phase transition in $Ni_{50}Mn_{34}In_{16}$ alloy. The width of the transition (see figure 1) suggests that the transition is broadened by quenched disorder, probably created during alloy formation. The disorder-influenced broadening of a first-order transition leads to a distribution of transition temperatures over the sample volume [34]. As a result, the phase transition line then broadens into a band [35–37]. The understanding of this phenomenon is especially important in the case of a martensitic transition because of the strong dependence of the martensitic transition temperature on composition [38]. The austenite to martensite transition region in $Ni_{50}Mn_{34}In_{16}$ alloy

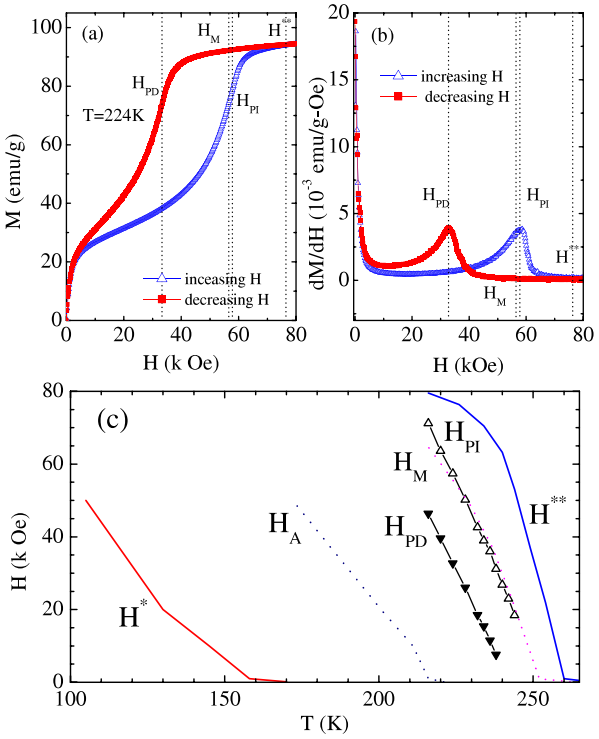

Figure 4. Isothermal magnetization (M) versus field (H) plot at 224 K for $Ni_{50}Mn_{34}In_{16}$ alloy (a) and the corresponding dM/dH versus H plot (b). The dotted lines denote the value of the characteristic field values on the field axis. (c) Temperature dependence of various characteristic fields across the martensitic transition in the $Ni_{50}Mn_{34}In_{16}$ alloy. See the text for details.

with the lowering of temperature (see figure 1) extends from the temperature of martensite start (T_{MS}) to the temperature of martensite finish (T_{MF}). As T decreases from T_{MS} to T_{MF}, the martensite phase fraction increases from 0 to 1 and the austenite phase fraction decreases from 1 to 0 [39]. Similarly the martensite to austenite phase transition with increasing temperature extends from the temperature of austenite start (T_{AS}) to the temperature of austenite finish (T_{AF}). Coexistence of martensite and austenite phases is observed in the T ranges T_{MS}–T_{MF} and T_{AS}–T_{AF}. The temperatures T_{MF} and T_{AF} are, respectively, the limits of supercooling (of the austenite phase) and superheating (of the martensite phase) [22]. Note that in the $Ni_{50}Mn_{34}In_{16}$ alloy T_{MS}, T_{MF}, T_{AS} and T_{AF} decrease with increasing field [14–19].

Similar to the case of a temperature-driven transition, the field-driven transition will also have a band of transition fields in the presence of disorder leading to a region of phase coexistence [37]. This is visible in figure 2 where the martensite to austenite as well as austenite to martensite transition occurs isothermally over a width of applied field. We therefore characterize the field-induced disorder broadened first-order magnetic transition in $Ni_{50}Mn_{34}In_{16}$ alloy by defining the characteristic fields of the transition. Figures 4(a) and (b) present the M versus H curve and the corresponding dM/dH versus H curve at a representative temperature 224 K. When 224 K is approached from 300 K in zero field, both the martensite and austenite phases are present in the sample as this temperature is lower than the T_{MS} but higher than T_{MF} in zero field [14, 18]. Now, as the field increases M increases towards saturation due to domain alignment (martensite and austenite phases are ferromagnetic in nature) and dM/dH decreases. Further increase in field leads to the transformation of the initial martensite phase to the austenite and as a result M as well as dM/dH increases (it has been discussed earlier that the austenite phase has a higher M value than the martensite phase). At a certain field, the rate of the martensite to austenite phase transformation is maximum. This gives rise to a peak in dM/dH, and this field value is marked as H_{PI}. At sufficiently high field, the martensite to austenite phase transition is complete and $M(H)$ reaches saturation. Above this field value, $M(H)$ and dM/dH for the increasing field cycle are indistinguishable from those for the decreasing field cycle. This field value is marked as H^{**} and is the limit of metastability (superheating [22]) of the martensite phase at this temperature. As the field is now decreased, the austenite phase is stable up to a field marked as H_M where the start of the austenite to martensite phase transition is accompanied by a decrease in M and a corresponding increase in dM/dH. At certain lower field values, the rate of transformation from the austenite to martensite phase is maximum. This produces a peak in dM/dH and this field value is marked as H_{PD}. As the field decreases to zero, we are back in the phase coexistence regime because the austenite to martensite phase transition is not completed in zero field at $T > 170$ K (this temperature has been estimated from low field M–T results [18]). It may be observed that figure 4(a) or 4(b) cannot give the estimate of the field H_A corresponding to the start of the martensite to austenite transition with increasing field because in zero field, at the beginning of the field-increasing experiment, we are already in the phase coexistence region. Similarly at the end of the field-decreasing experiment, in zero field, the sample is again in the phase coexistence region and we cannot reach the field H^*, the limit of metastability (supercooling [22]) of the austenite phase. H_A and H^* can be estimated from the $M(H)$ curves for temperatures below 170 K where only the martensite phase exists in zero field. However, the characteristic fields H_M, H^*, H_A and H^{**} can also be estimated from the $M(T)$ results obtained in various constant applied magnetic fields as the curves $H_M(T)$, $H^*(T)$, $H_A(T)$ and $H^{**}(T)$ should be identical to the curves $T_{MS}(H)$, $T_{MF}(H)$, $T_{AS}(H)$ and $T_{AF}(H)$, respectively. The temperature dependence of the characteristic fields H_M, H^*, H_A and H^{**}, or the field dependence of the characteristic temperatures T_{MS}, T_{MF}, T_{AS} and T_{AF}, constitute the H–T phase diagram of the alloy. In figure 4(c) we present the temperature dependence of the characteristic field values of the first-order transition in $Ni_{50}Mn_{34}In_{16}$ alloy, determined from the isothermal $M(H)$ curves and the constant field $M(T)$ results. This H–T phase diagram differs somewhat from that determined from the temperature dependence of resistivity in different applied fields [14] and this might be because of the different dynamical response of the two observables (magnetization and resistivity) near the start and finish of the transition. It is observed in figure 4(c) that, while the H_{PI} curve is closer to H^{**} as compared to the H_A curve, the H_{PD} curve lies closer to H_M as compared to H^*. This is related to

the shape of the $M(H)$ curves with increasing and decreasing fields across the transition (figure 2).

We note in figure 4(c) that H_{PI} and H_{PD} have approximately linear T dependence. Earlier, while analysing the field-induced first-order magnetic transitions with the help of the negative slope of the H/M versus M^2 curves [2], the characteristic field H_{PI} was predicted to increase with temperature [7]. Such temperature dependence of the characteristic fields was observed in the first-order paramagnetic–ferromagnetic phase transitions in various systems like manganites [7], NiMnGa [9], MnAs [26], $Gd_5Si_{1.7}Ge_{2.3}$ [40] and also in the ferromagnetic–ferromagnetic phase transition in NiMnGa [9]. But H_{PI} as well as all the other characteristic fields of $Ni_{50}Mn_{34}In_{16}$ alloy exhibit a totally different T dependence, e.g. they have a negative slope. The negative slope of the characteristic field in $Ni_{50}Mn_{34}In_{16}$ alloy is related to the fact that transition temperature in $Ni_{50}Mn_{34}In_{16}$ alloy shifts towards lower T with increasing field. Similar T dependence of the characteristic fields has been observed across the antiferromagnetic–ferromagnetic transition in Ru-doped $CeFe_2$ alloys [41].

3.5. Analysis of the slope of the H/M versus M^2 plots and the temperature dependence of the characteristic fields

Here we offer a possible explanation for the above observations in the $Ni_{50}Mn_{34}In_{16}$ alloy. It is worthwhile noting that the criterion of negative slope in the H/M versus M^2 isotherms was inferred from the theory of first-order magnetic transitions, where spontaneous magnetization is the appropriate order parameter. In the case of NiMnGa [9], spontaneous magnetization is the relevant order parameter for the first-order paramagnetic–ferromagnetic transition. But spontaneous magnetization is not the suitable order parameter for the first-order transition from one ferromagnetic to another ferromagnetic phase in $Ni_{50}Mn_{34}In_{16}$ alloy. However, irrespective of this difference, an ideal first-order magnetic transition should exhibit a discontinuity in magnetization [23]. If M increases discontinuously (or very sharply) across the transition with increasing H, the slope of H/M versus M^2 curves would become negative. In the case of a disorder-broadened first-order transition this discontinuity smears out [34]. The present experimental data and similar results on NiMnGa [9] suggest even in the case of broadened first-order transition the increase of M with increasing H becomes comparatively faster in the transition region. This results in a decrease in the slope of the H/M versus M^2 curves, and the decrease may or may not lead to a negative slope in the H/M versus M^2 isotherm. In $Ni_{50}Mn_{34}In_{16}$, starting from a temperature (300 K in the protocol adopted for measurement of isothermal M–H curves) well above the martensitic transition region, as the temperature is decreased the phase fraction of martensite (austenite) phase increases (decreases) from 0 to 1 (1 to 0) as the temperature decreases from T_{MS} to T_{MF} [39]. This martensite phase transforms back to the austenite phase under the application of field. The increase in M with increasing H because of this field-induced transition would depend upon the amount of initial martensite phase (at $H = 0$) as well as the difference in M between the martensite and austenite phases. The martensite and austenite phases in the $Ni_{50}Mn_{34}In_{16}$ alloy have a large difference in M (because of reasons discussed earlier). Also the amount of martensite phase formed, in the temperature region T_{MF}–T_{MS}, decreases with increasing temperature (see figure 4(c)). At lower temperatures (within the T range T_{MF}–T_{MS}), the initial amount of martensite phase formed is larger and the field-induced martensite to austenite transition gives larger change in M with increasing H and this effectively makes the slope of the H/M versus M^2 isotherm negative. The closer the temperature is to T_{MS}, the relatively smaller is the amount of martensite phase formed initially. With smaller initial martensite phase fraction, the field-induced transition becomes less effective in changing the slope of the H/M versus M^2 isotherms.

Now we investigate the possible cause of negative slope in temperature dependence of the characteristic fields H_M, H_{PD}, H^*, H_A, H_{PI} and H^{**} in $Ni_{50}Mn_{34}In_{16}$. In systems where the characteristic field increases with temperature [7, 9, 26, 40], the higher temperature phase has lower magnetization value. On the other hand, in $Ni_{50}Mn_{34}In_{16}$ the lower temperature phase (martensite) has lower magnetization. Similarly, in case of the first-order antiferromagnetic–ferromagnetic transition in Ru-doped $CeFe_2$ [8, 32, 41] the lower temperature antiferromagnetic phase has lower magnetization, and therefore the characteristic fields have a negative slope in the T dependence. In fact these results are in accord with the Clausius–Clapeyron equation for a first-order magnetic transition [26]:

$$\left(\frac{dT}{dH}\right)_P = -\frac{T\Delta M}{L}. \tag{2}$$

Here $L = T\Delta S$, ΔS being the entropy change during the transition. Applying equation (2) in the case of a field-induced first-order magnetic transition we find that, if the higher (lower) temperature phase has a higher (lower) magnetization value, then the transition temperature will decrease with increasing field, and as a result the characteristic fields for the isothermal transition will have negative temperature dependence.

To investigate more into the temperature dependence of the characteristic fields (or the field dependence of the characteristic temperatures) of $Ni_{50}Mn_{34}In_{16}$ a quantitative analysis of equation (2) was performed. It is noted that equation (2) has been used earlier to investigate the field dependence of transition temperatures in $Ni_{50}Mn_{34}In_{16}$ and other members of the Ni–Mn–In alloy family [11, 13]. For the present $Ni_{50}Mn_{34}In_{16}$ alloy, ΔS across the martensite–austenite transition was estimated earlier from differential scanning calorimetry (DSC) results [14]. Integrating the DSC curve between T_{MS} and T_{MF}, it was found that, for this alloy sample, $\Delta S = 2.9$ mJ g^{-1} K^{-1} across the austenite to martensite (cooling) transition [14]. Further, ΔM across the martensite–austenite transition was estimated from the difference in saturation magnetization (extrapolated) in the austenite and martensite phases. The lines fitted to the M versus T data obtained in the 50 kOe magnetic field (see insets to figure 1) were used for this purpose. We recall that equation (2) is defined for an ideal first-order transition with a unique transition temperature [23]. For a disorder-broadened

first-order transition there is a landscape of transition temperatures [34–37], and this makes the straightforward application of equation (2) difficult. The same landscape picture [34–37] also leads to uncertainty in the estimation of ΔM, because ΔM determined through extrapolation depends on the temperature where it is determined. Putting $T = T_{MS}$ in equation (2), we get $dT/dH = 0.52$ K kOe^{-1} while the dT/dH determined from the slope of the linear portion of the H_M curve (figure 4(c)) comes out to be 0.46 K kOe^{-1}. But if we take T_{MF} as the T in equation (2) then we get $dT/dH = 0.55$ K kOe^{-1}, while dT/dH determined from the average slope of the H^* curve is found to be 1.08 K kOe^{-1}. For the martensite to austenite (heating) transition, dT/dH is found to be 0.48 and 0.44 K kOe^{-1}, respectively, by taking $T = T_{AS}$ and T_{AF} in equation (2). But the same slopes corresponding to the linear portions of the H_A and H^{**} curves (figure 4(c)), respectively, are found to be 0.95 and 0.32 K kOe^{-1}. On the other hand, dT/dH estimated from the slopes of the H_{PD} and H_{PI} curves, respectively, come out to be 0.57 and 0.54 K kOe^{-1}. Thus it appears that in the case of the disorder-broadened first-order transitions [34], though the Clausius–Clapeyron equation predicts the nature of the slope of the phase transition lines, an exact quantitative result is rather difficult to obtain.

4. Conclusion

The isothermal M versus H curves of $Ni_{50}Mn_{34}In_{16}$ show the signatures of a field-induced first-order martensite to austenite phase transition in the temperature range 200–250 K. The isothermal H/M versus M^2 curves, however, do not exhibit a negative slope at certain temperatures within this temperature range. This suggests that the criterion of relating the negative slope of the H/M versus M^2 isotherms to the first-order magnetic transitions is not applicable for all the magnetic transitions. On the other hand, a decrease in slope of the H/M versus M^2 isotherm is found to characterize the first-order magnetic transition in the present case. Such a decrease in slope might lead to a negative slope of the H/M versus M^2 isotherms if there is a large change of magnetization because of the field-induced magnetic phase transition. The isothermal $M(H)$ curves and the temperature dependence of the characteristic fields of the first-order martensite–austenite transition can be explained within the framework of disorder-broadened first-order transition. The nature of the temperature dependence of the characteristic fields is found to follow the Clausius–Clapeyron relation for a first-order phase transition.

References

[1] Aharoni A 1996 *Introduction to the Theory of Ferromagnetism* (Oxford: Clarendon)
[2] Banerjee S K 1964 *Phys. Lett.* **12** 16
[3] Mira J, Rivas J, Rivadulla F and Lopez-Quintela M A 2002 *Physica* B **320** 23
[4] Mira J, Rivas J, Rivadulla F, Vazquez C V and Lopez-Quintela M A 1999 *Phys. Rev.* B **60** 2998
[5] Otero-Leal M, Rivadulla F and Rivas J 2007 *Phys. Rev.* B **76** 174413
[6] Rivadulla F, Rivas J and Goodenough J B 2004 *Phys. Rev.* B **70** 172410
[7] Amaral V S, Araujo J P, Pogerelov Y G, Tavares P B, Sousa J B and Vieira J M 2002 *J. Magn. Magn. Mater.* **242–245** 655
[8] Jiang W, Zhou X, Kunkel H and Williams G 2008 *J. Magn. Magn. Mater.* **320** 2144
[9] Zhou X, Li W, Kunkel H P and Williams G 2006 *Phys. Rev.* B **73** 012412
[10] Sutou Y, Imano Y, Koeda N, Omori T, Kainuma R, Ishida K and Oikawa K 2004 *Appl. Phys. Lett.* **85** 4358
[11] Oikawa K, Ito W, Ymano Y, Sutou Y, Kainuma R, Ishida K, Okamoto S, Kitakami O and Kanomata T 2006 *Appl. Phys. Lett.* **88** 122507
[12] Krenke T, Acet M, Wassermann E F, Moya X, Manosa L and Planes A 2006 *Phys. Rev.* B **73** 174413
[13] Yu S Y, Liu Z H, Liu G D, Chen J L, Cao Z X, Wu G H, Zhang B and Zhang X X 2006 *Appl. Phys. Lett.* **89** 162503
[14] Sharma V K, Chattopadhyay M K, Shaeb K H B, Chouhan A and Roy S B 2006 *Appl. Phys. Lett.* **89** 222509
[15] Sharma V K, Chattopadhyay M K and Roy S B 2007 *J. Phys. D: Appl. Phys.* **40** 1869
[16] Krenke T, Duman E, Acet M, Wassermann E F, Moya X, Manosa L, Planes A, Suard E and Ouladdiaf B 2007 *Phys. Rev.* B **75** 104414
[17] Moya X, Mañosa L, Planes A, Aksoy S, Acet M, Wassermann E F and Krenke T 2007 *Phys. Rev.* B **75** 184412
[18] Sharma V K, Chattopadhyay M K, Kumar R, Ganguli T, Tiwari P and Roy S B 2007 *J. Phys.: Condens. Matter* **19** 496207
[19] Sharma V K, Chattopadhyay M K and Roy S B 2007 *Phys. Rev.* B **76** 140401(R)
[20] Kuz'min M D 2005 *Phys. Rev. Lett.* **94** 107204
[21] Kuz'min M D, Chernyshov A S, Pecharsky V K, Gschneidner K A Jr and Tishin A M 2006 *Phys. Rev.* B **73** 132403
[22] Chaikin P M and Lubensky T C 1995 *Principles of Condensed Matter Physics* (Cambridge: Cambridge University Press)
[23] White R M and Geballe T H 1979 *Long Range Order in Solids* (New York: Academic)
[24] Krenke T, Duman E, Acet M, Wassermann E F, Moya X, Manosa L and Planes A 2005 *Nat. Mater.* **4** 450
[25] Brown P J, Gandy A P, Ishida K, Kainuma R, Kanomata T, Neumann K U, Oikawa K, Ouladdiaf B and Ziebeck K R A 2006 *J. Phys.: Condens. Matter* **18** 2249
[26] Bean C P and Rodell D S 1962 *Phys. Rev.* **126** 104
[27] Campbell A J, Paul D M K and McIntyre G J 2000 *Phys. Rev.* B **61** 5872
[28] Pecharsky V K, Horn A P, Gschneidner K A Jr and Rink R 2003 *Phys. Rev. Lett.* **91** 197204
[29] Zhang Y Q, Zhang Z D and Aarts J 2004 *Phys. Rev.* B **70** 132407
[30] Manekar M, Chaudhary S, Chattopadhyay M K, Singh K J, Roy S B and Chaddah P 2002 *J. Phys.: Condens. Matter* **14** 4477
[31] Roy S B, Perkins G K, Chattopadhyay M K, Nigam A K, Sokhey K J S, Chaddah P, Caplin A D and Cohen L F 2004 *Phys. Rev. Lett.* **92** 147203
[32] Chattopadhyay M K, Manekar M A and Roy S B 2006 *J. Phys. D: Appl. Phys.* **39** 1006
[33] Bhobe P A, Priolkar K R and Nigam A K 2007 *Appl. Phys. Lett.* **91** 242503
[34] Imry Y and Wortis M 1979 *Phys. Rev.* B **19** 3580
[35] Manekar M A, Chaudhary S, Chattopadhyay M K, Singh K J, Roy S B and Chaddah P 2001 *Phys. Rev.* B **64** 104416

[36] Roy S B and Chaddah P 2004 *Phase Transit.* **77** 767
[37] Chattopadhyay M K, Roy S B, Nigam A K, Sokhey K J S and Chaddah P 2003 *Phys. Rev.* B **68** 174404
[38] Kartha S, Krumhansl J A, Sethna J P and Wickham L K 1995 *Phys. Rev.* B **52** 803
[39] Guenin G 1989 *Phase Transit.* **14** 165
[40] Tegus O, Bruck E, Zhang L, Dagula, Buschow K H J and de Boer F R 2002 *Physica* B **319** 174
[41] Chattopadhyay M K and Roy S B 2008 *J. Phys.: Condens. Matter* **20** 025209